



Preparation of mesoporous silica nanocapsules with a high specific surface area by hard and soft dual templating approach: Application to biomass valorization catalysis

Tommy Haynes^a, Oujidane Bounouch^a, Vincent Dubois^b, Sophie Hermans^{a,*}

^a IMCN Institute, MOST Division, Université catholique de Louvain, 1 Place Louis Pasteur, B-1348, Louvain-la-Neuve, Belgium

^b Department of Physical Chemistry and Catalysis, LABIRIS, 1 Avenue Emile Gryson, 1070, Brussels, Belgium

ARTICLE INFO

Keywords:

Nanocapsules
Mesoporous silica
Carbon black
Carbon nanofiber
Soft templating
Hard templating

ABSTRACT

Mesoporous silica nanocapsules were prepared by a soft and hard dual templating approach. Carbon black and carbon nanofibers, used as sacrificial templates (hard template) have been coated by a mesoporous silica layer. Pluronic (P123/F127) and cetrimonium bromide were selected as surfactants (soft template) to produce mesoporous layers with different morphologies and pore sizes. The coated samples were then calcined at high temperature to remove the hard template and produce silica nanocapsules with mesopores in their walls. The so-obtained materials have been characterized by XPS, elemental analyses (ICP), TEM, N₂ physisorption and XRD. The results have shown that the obtained materials exhibit a high specific surface area and a short diffusional pathway within the porous structure, which represents a significant advantage for catalysis applications. Finally, mesoporous acidic nanocapsules were prepared by sulfonic acid moieties grafting, and were tested as a catalyst in a biomass valorization reaction, the hydrolysis of cellobiose. The catalysts have shown high catalytic performances underlining the high potential of the present synthetic approach to produce versatile mesoporous materials.

1. Introduction

Since the discovery of mesoporous molecular sieves (MMS) in 1992 by the Mobil Company [1,2], the preparation of mesoporous silica materials has attracted great interest in the scientific community due to their unique properties, particularly in comparison with microporous zeolites and zeotypes. Mesopores allow faster diffusion of liquid and gases through the material. In the last few years a significant number of reviews have emerged with illustrations of very wide application fields such as adsorption, separation, sensors, drug delivery and catalysis [3–6]. A recent trend is the control of particle size and shapes from the macroscopic down to the nanometer range to allow even shorter diffusional pathways. Although there is a large variety of mesoporous silica morphologies, the most frequently encountered are spheres [7–15] and tubes [16–21]. Regardless the application field, the main required property of these materials is a high specific surface area. In catalysis, mass transfer is a very important parameter as the active sites, such as metallic nanoparticles, are usually dispersed within the mesoporous framework. Unfortunately the diffusion pathway is usually long inside

mesoporous materials (with μm particles) leading to a drastic loss of performance. Therefore the control of mesoporous materials thickness and morphology is a big challenge for catalytic applications.

Two common methods are widespread to produce mesoporous silica materials: the soft and hard templating syntheses [22]. In the soft templating approach, a surfactant or amphiphilic block copolymer directs the mesoporous material synthesis by forming micelles in solution, around which the silica precursor will be polymerized under hydrothermal conditions [23]. The soft template is therefore self-assembled within the reaction medium and allows the production of nanomaterials with various structures depending on many parameters such as the temperature or pH [24]. In the hard templating approach, a previously prepared mesoporous solid template material such as mesoporous carbon [25] is used. The rigid template directly determines the material morphology.

However, although the templated approaches based on soft- or hard-templating are still the most effective and popular techniques for the preparation of mesoporous materials, they are subject to some limitations. For example, in the soft templating approach, the control of

* Corresponding author.

E-mail address: sophie.hermans@uclouvain.be (S. Hermans).

particle size and morphology is difficult owing to the sensitivity of the sol-gel process [26]. As an alternative, hard/soft dual templating approaches have been developed. Recently, hollow mesoporous silica nanoparticles have been successfully prepared via this method and explored for drug delivery and protein adsorption [27]. Bian et al. have also reported an important paper on the preparation of mesoporous silica tubes with different internal morphologies by this way [18]. Nevertheless, in both studies, CTAB was systematically used as soft template. Moreover, although different nanofibers-like structures were used as hard template in Bian's study, the same experimental procedure was applied without modifying any other parameters to investigate their influence on morphology or textural properties of synthesized materials.

In this context, we report here a methodology to produce mesoporous silica nanocapsules of two types, namely mesoporous silica nanofibers [mSNF] and mesoporous silica nanospheres [mSN], using hard and soft dual templates. To demonstrate that the methodology developed herein can be generalized and allows the production of a large range of mesoporous materials, three experimental variables have been modified: the pH (acid/basic), the soft template nature and the hard template structure. Cetyltrimethylammonium bromide (CTAB) and pluronic F127/P123 have been respectively selected as ionic and neutral soft templates. Two hard templates, carbon black (CB) and carbon nanofibers (CNF), with very different morphologies, have been chosen as starting templating structures, to give spherical [mSN] and fibrous [mSNF] materials, respectively. Finally, an acidic material [mSN-SO₃H] was prepared from the mesoporous nanocapsules, as an illustrative application. Currently, depolymerisation of cellulose is known to be a very challenging reaction that needs to be investigated further for economic reasons [28]. Due to the high crystallinity and low solubility of cellulose, many studies are carried out on cellobiose, a disaccharide considered as the simplest model-molecule of cellulose [29]. Indeed, cellulose depolymerisation consists mainly in breaking the β-1,4-glycosidic bonds between the sugar units. This hydrolysis reaction requires strong acid surface sites if carried out with a catalyst, to be as efficient as mineral acids in stoichiometric amounts. Therefore, our acidic mSN-SO₃H material was tested as catalyst in the cellobiose hydrolysis reaction, considered as a very important model reaction for cellulose valorization.

2. Experimental

2.1. Reagents and materials

The carbon black (CB) was received as 250G type from IMERYS GRAPHITE & CARBON. Pyrograf III PR-24-XT-LHT-OX (CNF) were supplied by Applied Sciences Inc. (USA). Hexadecyltrimethylammonium bromide (CTAB, 95%), (3-aminopropyl)trimethoxysilane (APTES, 99%), tetraethyl orthosilicate (TEOS, >98%), thionyl chloride (SOCl₂, >99%), (3-Mercaptopropyl)triethoxysilane (MPTMS, 95%), pluronic F127 and pluronic P123 were purchased from Sigma Aldrich and used as received. Hydrogen peroxide, 35% w/w was purchased from Alfa Aesar. A commercial ultrasonic cleaner (VWR) was used for sonication.

2.2. Syntheses

2.2.1. Synthesis of CB@mSiO₂(C)

The synthesis of carbon black (CB) covered by a thin mesoporous silica layer, noted CB@mSiO₂(C), has been previously described by us [30]. Carboxylic acid groups existing on the CB (2 g) surface were chlorinated in refluxing SOCl₂ (6 mL of thionyl chloride in 100 mL of toluene). After this acylation reaction, the resulting material (1g) was introduced in a 250 mL round-bottom flask containing 100 mL of dichloromethane and 1 mL of APTES ((3-aminopropyl)triethoxysilane) was added to produce a robust amide bond. Then the mesoporous silica layer was synthesized by TEOS (0.7 mL) hydrolysis in alkaline solution

(10 mL of NaOH (0.1 M) in 25 mL of water) at 60 °C with CTAB (0.571 g) as template. Finally the solid was washed in refluxing ethanol (250 mL) and dried at 100 °C overnight to produce the desired material CB@mSiO₂(C).

2.2.2. Synthesis of CNF@mSiO₂(C)

The synthesis of CNF@mSiO₂(C) was achieved following the same procedure as described above for CB@mSiO₂(C), using 1 mL of TEOS added dropwise instead of 0.7 mL.

2.2.3. Synthesis of CNF@mSiO₂(F)

2 g of carbon nanofibers (CNF) were introduced in a 250 mL round-bottom flask containing 100 mL of toluene. 6 mL of SOCl₂ were added and the mixture was heated for 5 h under reflux (120 °C). Then, it was filtered out and extensively washed with toluene (500 mL). The resulting material (noted CNF-Cl) was dried overnight under vacuum at 100 °C. 1 g of CNF-Cl was introduced in a 250 mL round-bottom flask containing 100 mL of dichloromethane. 1 mL of APTES was added and the mixture was stirred for 24 h at room temperature. The material (CNF-APTES) was filtered out, washed with dichloromethane (250 mL) and methanol (250 mL) and dried overnight under vacuum at 100 °C. Then, 0.250 g of CNF-APTES was introduced in a 100 mL round bottom flask containing 35 mL of HCl (3.10⁻³ M) acidic solution and the mixture was sonicated for 10 min. To this suspension 60 mg of F127 were added and the solution was heated at 60 °C. 1 mL of TEOS was added dropwise within 30 min. This suspension was further stirred for 3h30, and then charged into a polypropylene bottle, which was closed tightly and heated at 100 °C for 3 days. The product was filtered out, washed with ethanol (250 mL) and dried at 100 °C overnight. The F127 template was removed by refluxing in ethanol the obtained solid material noted CNF@mSiO₂(F).

2.2.4. Synthesis of CB@mSiO₂(P)

The synthesis of CB@mSiO₂(P) was achieved following the procedure used to prepare CNF@mSiO₂(F), with three modifications. First, HCl 0.3 M was used instead of HCl 3.10⁻³ M. Second, 120 mg of pluronic P123 were added instead of 60 mg of F127. Finally, 0.55 mL of TEOS was added dropwise within 30 min.

2.2.5. Synthesis of mesoporous nanocapsules

The preparation of the final mesoporous silica materials is based on the combustion under air of the carbonaceous solid (CB or CNF) covered by the thin mesoporous silica layer. In a typical procedure, CB@mSiO₂ or CNF@mSiO₂ samples were placed into porcelain combustion boats and heated at 600 °C during 24h under air (GSM11/8 CARBOLITE) to produce two types of nanocapsules: mesoporous silica nanospheres (mSN(C) and mSN(P)) and mesoporous silica nanofibers (mSNF(C) and mSNF(F)). During calcination residual surfactant is also removed.

2.2.6. Synthesis of sulfonic acid-functionalized mesoporous nanocapsules - mSN(C)-SO₃H

500 mg of mesoporous material (mSN(C)) was introduced in a 500 mL round bottom flask containing 250 mL of toluene. Then 1.25 mL of (3-mercaptopropyl)trimethoxysilane (MPTMS) were added and the mixture was vigorously stirred under reflux for 24 h. The product, namely mSN(C)-SH, was filtered out, washed with 400 mL of toluene and dried at 100 °C overnight. The material was then dispersed in a mixture of methanol (200 mL) and hydrogen peroxide 35% (100 mL) and stirred for 24 h. Finally, the solid was filtered out, washed with 500 mL of distilled water and dried at 100 °C overnight to give the desired product mSN(C)-SO₃H.

2.3. Characterization

The solid materials were characterized by X-ray photoelectron spectroscopy (XPS), elemental analyses (ICP), transmission electron microscopy (TEM), Boehm titration, X-ray powder diffraction (XRD) and

N₂ physisorption.

XPS analyses were carried out at room temperature with a SSI-X-probe (SSX 100/206) photoelectron spectrometer from Surface Science Instruments (USA), equipped with a monochromatized microfocus Al X-ray source. Samples were stuck onto small sample holders with double-face adhesive tape and then placed on an insulating ceramic carousel (Macor®, Switzerland). Charge effects were avoided by placing a nickel grid above the samples and using a flood gun set at 8eV. The binding energies were calculated with respect to the C-(C, H) component of the C1s peak fixed at 284.8 eV. Data treatment was performed using the CasaXPS program (Casa Software Ltd., UK). The peaks were decomposed into a sum of Gaussian/Lorentzian (85/15) after subtraction of a Shirley-type baseline.

The elemental analyses (C, H, N, Si, Fe, Ni, Co) were carried out by MEDAC Ltd., UK, by microgravimetry for C, H, N (direct measure) and by ICP after acid digestion for Si, Fe, Ni and Co.

TEM images were obtained on a LEO 922 Ω Energy Filter Transmission Electron Microscope operating at 120 kV. The samples were suspended in hexane under ultrasonic treatment. A drop of the suspension was deposited on a holey carbon film supported on a copper grid (Holey Carbon Film 300 Mesh Cu, Electron Microscopy Sciences), which was dried overnight under vacuum at room temperature, before introduction in the microscope. To evaluate the materials mechanical strength, 20 mg of sample were also finely grinded in a mortar before the TEM grid preparation.

Boehm titration method was used to evaluate the materials acidity. NaOH solutions were prepared by dilution of Titrisol ampoules (VWR) containing precise and known quantities of sodium hydroxide. HCl solutions were prepared by the dilution of concentrated hydrochloric acid. The HCl concentrations were determined by titration with the standard NaOH solution. These solutions were prepared with mQ water that had been previously decarbonated by argon flushing. For titrating the acid groups, 60 mg of sample were dispersed in 30 mL of NaOH 0.01 mol/L and the solution was decarbonized for 1 h under N₂ flux. The mixture was then agitated for 23 h under N₂ atmosphere. The suspension was then filtrated and two times 10 mL of the resulting filtrate were back-titrated, under N₂ flux, using the HCl 0.005 mol/L solution. The indicator used is phenolphthalein. The amount of acid functions in the material is determined by calculating the difference between the initial amount of NaOH and the amount of NaOH titrated by the HCl.

The pore texture of the mesoporous materials was characterized by nitrogen adsorption-desorption isotherms. The measurements were achieved by using a Micromeritics ASAP 2020 analyzer at 77K. Before analysis, the samples (0.02–0.10 g) were degassed for 2 h at 200 °C with a heating rate of 10 °C/min under 0.133 Pa pressure. The analysis of the isotherms provided specific surface areas calculated with the Brunauer-Emmett-Teller (BET) equation, S_{BET} . The pore volume, V_p , of the samples and the pores average diameter were calculated using the Barrett-Joyner-Halanda (BJH) and DFT models.

Powder X-ray diffraction was performed on a Bruker D8 advanced diffractometer with a Bragg Brentano geometry, using a LinkEye XE-T detector with Cu K α radiation ($\lambda = 0.15418$ nm) and a power of 1200 W (40 kV, 30 mA). The samples were scanned from 0.8 to 10 (2 theta range) at a scanning rate of 1.5°/min.

2.4. Catalytic tests

The tests were carried out in a 250 mL stainless steel Parr autoclave. 1g of cellobiose was added to 300 mg of catalyst in 120 mL of mQ water. Then, the autoclave was sealed and the system was purged three times with nitrogen. Once the desired temperature has been reached (130 °C), the mixture was stirred at 1700 rpm for 2 h. The system was then cooled down to room temperature and the solution was filtrated. The filtrate was then diluted to 250 mL with mQ water and analyzed by HPLC.

HPLC analyses were performed with a Waters system equipped with Waters 2414 refractive index (RI) detector (detector temperature = 30

°C). The column used is an Aminex HPX 87C column, with mQ H₂O (18 M Ω cm at 25 °C) as an eluent, a flux of 0.5 mL/min, a column temperature of 85 °C and 25 μ L of injected volume.

3. Results and discussion

As depicted in Fig. 1, carbon materials (CNF and CB) used as hard templates were covered by a thin mesoporous silica layer to produce CNF@mSiO₂ and CB@mSiO₂ samples. Three surfactants were used as soft templates in a comparative manner, namely pluronic F127, pluronic P123 and CTAB, to form the mesoporous silica layer by the sol-gel process in acidic or basic conditions. These surfactants are known to induce different pores sizes [30]. The soft template was firstly extracted from the four covered samples (CB@mSiO₂(C), CB@mSiO₂(P), CNF@mSiO₂(C), and CNF@mSiO₂(F)) by refluxing them in ethanol for 24h to prevent damaging structural changes of the mesoporous silica materials. Indeed, without this extraction step, the removal of both templates in high amounts by calcination leads to partial destruction of the mesoporous silica nanocapsules, as shown by the TEM images given in Electronic Supplementary Information (ESI 1). Then the samples were submitted to a calcination step to remove both hard and residual soft templates. The resulting materials, namely mSN(C), mSNF(C), mSN(P) and mSNF(F) were characterized by XPS, TEM, XRD and N₂ physisorption. Finally, sulfonic acid moieties were grafted on mSN(C) as an illustrative example, to produce a mesoporous acidic material, mSN(C)-SO₃H. After characterization, this material was tested as acidic catalyst in a biomass model-reaction: the hydrolysis of cellobiose to glucose.

3.1. XPS study

To confirm the formation of mesoporous silica materials (mSN or mSNF), XPS analyses were performed on initial carbonaceous materials (CB/CNF), covered materials (ESI 2) and final silica-only materials (mSN/mSNF) for each of the 4 combinations tested (Table 1). As expected, when the carbonaceous materials were covered by a mesoporous silica layer, we noticed a decrease in C1s surface atomic percentage and conversely an increase in O1s and Si2p atomic percentages (see ESI 2). It can also be observed that N1s atomic percentage increases after silica deposition for samples using the anionic surfactant. This is due to the persistence of residual CTAB template in porous silica channels even after the ethanol extraction step. In the same way, if we look at the O/Si ratio of covered samples, we observe that the CNF@mSiO₂(F) material displays the highest ratio. This is also attributed to the presence of residual F127 surfactant. After the combustion of carbon cores under air, the C1s atomic percentage drastically decreases to values near zero for each calcined material (Table 1). This result attests the silica-only material production, as ca. 1–4C1s at.% has reached the unavoidable carbon surface contamination rates (adventitious carbon) usually observed by XPS. This has been confirmed by elemental analysis by ICP (ESI 3). Furthermore, the O/Si ratio is close to 2 (corresponding to pure SiO₂) which demonstrates that hard and residual soft templates have been totally removed. This ratio is slightly higher for mSNF samples, which can be explained by the presence of iron oxide impurities (transition metal catalyst used in the catalytic chemical vapor deposition for carbon nanofibers production, see ESI 3). All the results obtained by XPS corroborate the production of silica materials as expected.

3.2. TEM study

Transmission electron microscopy imaging was performed after each synthesis step to assess the morphology of porous materials obtained (Fig. 2 and ESI 4). The TEM images clearly indicate that the silica layer is uniformly deposited on CB and CNF in comparison with uncovered starting templates (ESI 4). Moreover the silica layers show a well-developed porosity for each covered sample, but in the case of CNF@mSiO₂(F) and CB@mSiO₂(P) samples, the coating looks less

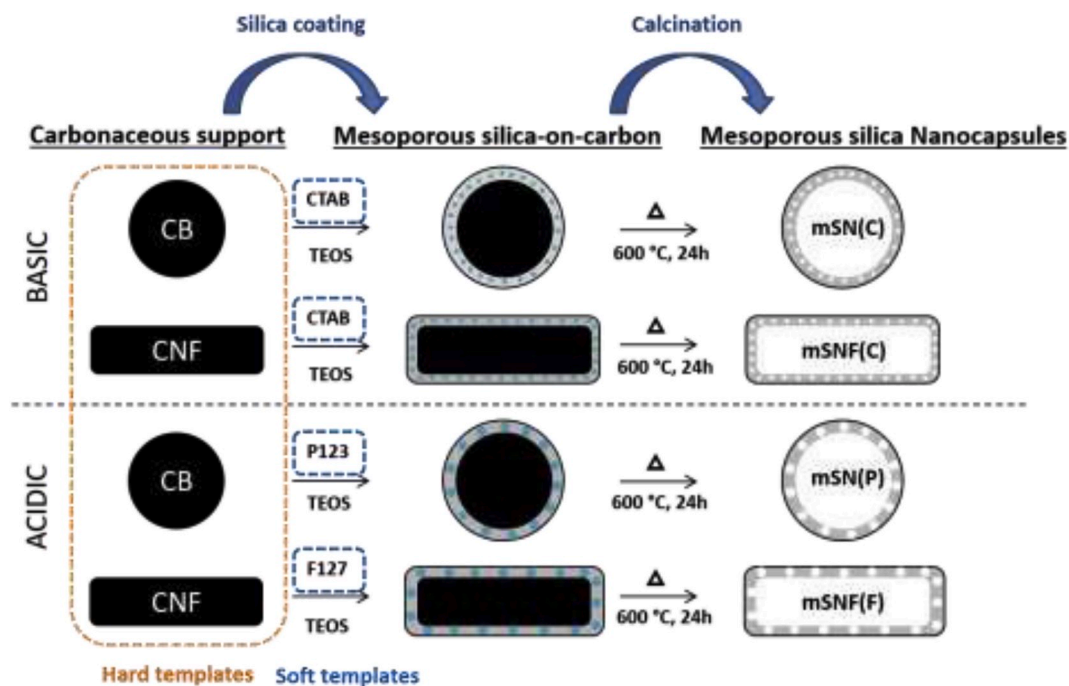


Fig. 1. Synthetic routes for mesoporous silica nanocapsules.

Table 1

XPS analyses of initial carbonaceous solids and mesoporous nanocapsules.

At. %	C1s	O1s	N1s	Si2p	O/Si
CB	96.8	2.9	0.2	/	/
mSN(C)	1.5	64.4	/	34.1	1.9
mSN(P)	1.2	64.8	/	34.0	1.9
CNF	94.6	5.3	0.1	/	/
mSNF(C)	2.7	68.4	/	28.9	2.4
mSNF(F)	4.1	66.6	/	29.2	2.3

regular with some protrusions. After calcination under air, hollow silica materials are produced as shown in Fig. 2. These materials maintain the carbon black or fibers structures and the pores are always recognizable. Irrespective of which conditions (acidic/basic), surfactant (CTAB/F127/P123), or carbonaceous solid template (CB/CNF) chosen, silica porous materials with structures very close to the starting hard templates were generated.

The nanocapsules materials were also finely grinded to evaluate their mechanical strength. As shown by TEM imaging (ESI 5), the materials maintained their original structure after grinding, which illustrates the robustness of our solids. From TEM images we also observe that the mesoporous walls of mSN and mSNF materials are not thicker than 30 nm. This is a very important result in term of mass transportation which is a critical parameter for future applications in catalysis. In the case of mesoporous nanospheres (mSN(C) and mSN(P)) this value is even smaller than 15 nm. This demonstrates the powerfulness of the developed methodology to prepare catalytic materials with small diffusional pathways.

3.3. XRD

The XRD patterns of final calcined samples are presented in Fig. 3. The mSN(C) diffractogram (Fig. 3, curve a) shows low angle peaks corresponding to (100), (110) and (200) reflections that are typical of the ordered MCM-41 hexagonal structure [31]. Compared with this material, the peaks obtained for mSNF(C)/(F) and mSN(P) materials (Fig. 3, curves b, c and d) are broader and less defined, meaning that the

silica materials are less ordered. This observation correlates with the protrusions observed onto the materials surface. Nevertheless, the strong peaks at $ca. 2\theta = 1.2^\circ$ for mSN(P)/mSNF(F) and 2.2° for mSNF(C) directly indicates the presence of MCM-41 and SBA-15/16 like-structures (SBA being the typical crystalline structure obtained with neutral surfactant) [24,32,33]. These results are not surprising because MCM and SBA syntheses are very sensitive and, as mentioned above, depend on many parameters [34,35]. The presence of hard templates in the reaction mixture makes it even more difficult to produce ordered mesoporous materials.

3.4. BET study

The nitrogen adsorption-desorption isotherms for materials derived from carbon black and carbon nanofibers with CTAB, F127 or P123 as a surfactant are shown in Fig. 4. As expected, the starting CB and CNF templates exhibit the curves of non-porous/macroporous materials, which is reflected in the low specific surface area ($63 \text{ m}^2/\text{g}$ and $26 \text{ m}^2/\text{g}$, respectively, Fig. 4). After the silica deposition (see ESI 6 for more details about covered samples) and then templates calcination, the specific surface area of mSN and mSNF materials increase drastically to reach values of $1213 \text{ m}^2/\text{g}$, $610 \text{ m}^2/\text{g}$, $1589 \text{ m}^2/\text{g}$ and $574 \text{ m}^2/\text{g}$ for mSN(C), mSN(P), mSNF(C) and mSNF(F), respectively (see Fig. 4). These increases are the result of a combination of factors: (i) hard and soft surfactants removal, (ii) gain of nanofiber/carbon black internal surface and (iii) release of closed pores that were connected to the nanofiber/carbon black surfaces but not accessible from the external silica surface. Moreover, the materials using CTAB as template (mSNF(C) and mSN(C)) disclose type IV isotherms corresponding to mesoporous materials with a slight increase around $P/P_0 \sim 0.4$ associated with capillary condensation in cylindrical pores. The nitrogen adsorption-desorption isotherms also show clearly H1 (mSN(C)), H4 (mSNF(C)) and H3 (mSNF(F) and mSN(P)) hysteresis loops according to IUPAC classification, implying materials possessing mesoporous frameworks with a very narrow (H1 and H4) or wide (H3) pore size distribution [24,35]. These results are verified in the BJH distributions (ESI 7) revealing a mean pores size centered at 1.3 nm and 1.5 nm for mSN(C) and mSNF(C) materials, respectively, and at 5.6 nm for mSNF(F) with a broader pore

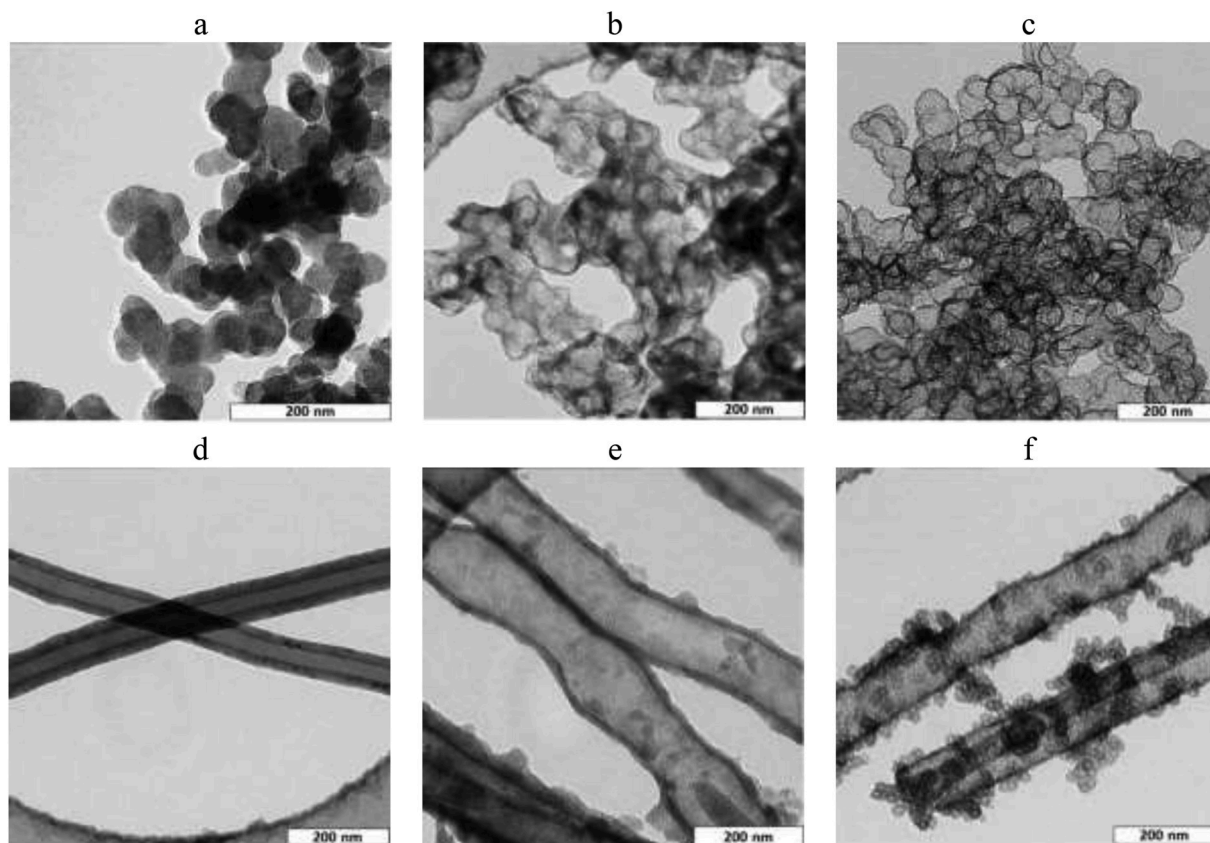


Fig. 2. TEM images of starting carbonaceous templates and porous silica materials after calcination: (a) CB (b) mSN(C) (c) mSN(P) (d) CNF (e) mSNF(C) and (f) mSNF(F).

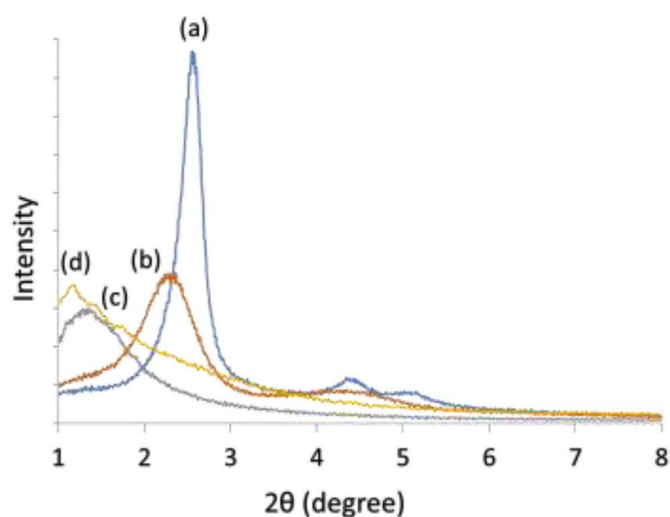


Fig. 3. Powder XRD patterns at small angles for (a) mSN(C), (b) mSNF(C), (c) mSNF(F) and (d) mSN(P) materials.

size distribution. Nevertheless, it was shown that the Kelvin equation based procedures, such as the BJH method, significantly underestimate the pore size for narrow mesopores which is the case for mSN(C) and mSNF(C) materials. To overcome this limitation, density functional theory (DFT) analyses are often applied [36]. As shown in ESI 8, the DFT data treatment reveals that mSN(C) and mSNF(C) both display mesopores sizes centered on 2.9 nm and 3.2 nm respectively. Although a high nitrogen uptake at low relative pressures ($P/P_0 < 0.1$) and DFT data treatment (see ESI 8) for these samples seem to indicate the presence of

micropores, it has been proven that MCM-41/48 are exclusively mesoporous materials [37,38]. In the case of mSN(P) material, it is quite difficult to determine precisely an average pore size (it is centered at ~ 5 nm) value due to the very large distribution of sizes observed (ESI 9). It has also been observed that the mean pore size is slightly smaller after the calcination step for mSN(C) and mSNF(C) materials. This is caused by shrinkage of the silica framework during the high temperature decarbonization. Based on XRD, BET and TEM analyses, we can conclude that the as-prepared silica materials show a well-structured nanoarchitecture with a very high specific surface area.

3.5. Catalytic application

The mesoporous silica nanospheres (mSN(C)) were tested as acidic catalyst in the conversion of cellobiose into glucose. To do so, sulfonic acid moieties were grafted on calcined mSN(C) according to a literature procedure [39] to produce an acidic material, namely mSN(C)-SO₃H. Briefly, this procedure consists in grafting thiol groups on the silica surface followed by their subsequent oxidation into sulfonic groups (Fig. 5). This catalyst has been characterized by XPS, TEM, Boehm titration and nitrogen physisorption.

For the mSN(C)-SH sample, the XPS spectrum discloses a S2p peak (1.6 at.%, see ESI 10 for complete quantitative analysis) corresponding to thiol groups (163.6 eV for S_{2p3/2}) [40], which corroborates the MPTMS grafting on nanocapsules surface. After the oxidation step with hydrogen peroxide, the S2p signal shifts towards higher binding energy, typical of sulfonic acid [40] (167.9 eV for S_{2p3/2}) (ESI 11). XPS also reveals that 78% of thiols groups have been effectively oxidized into sulfonic groups. TEM micrographs (ESI 12) showed that the anchoring of sulfonic acids does not change the morphology of our material, which remains nanocapsules. The total acidity of the mSN(C)-SO₃H catalyst

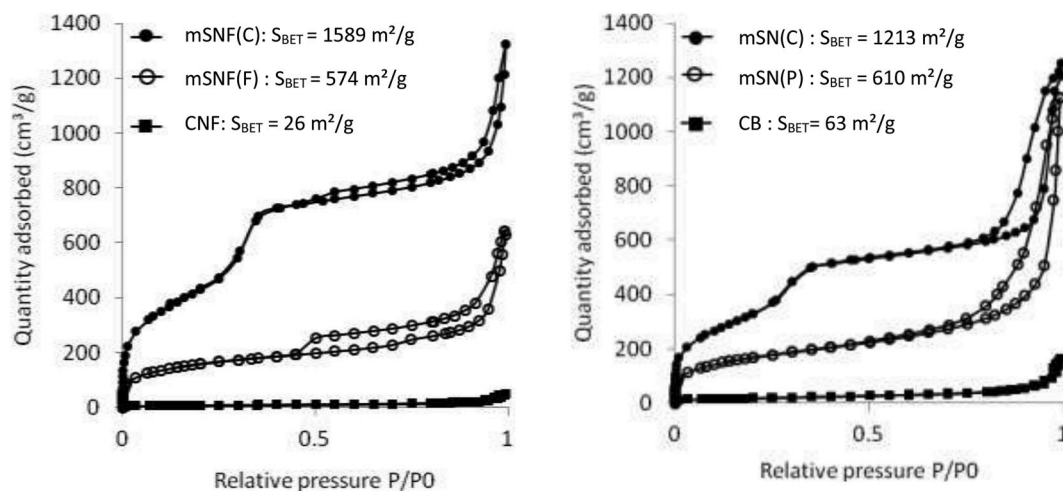


Fig. 4. Nitrogen adsorption-desorption isotherms at 77 K for carbonaceous templates (CNF and CB) and calcined materials.

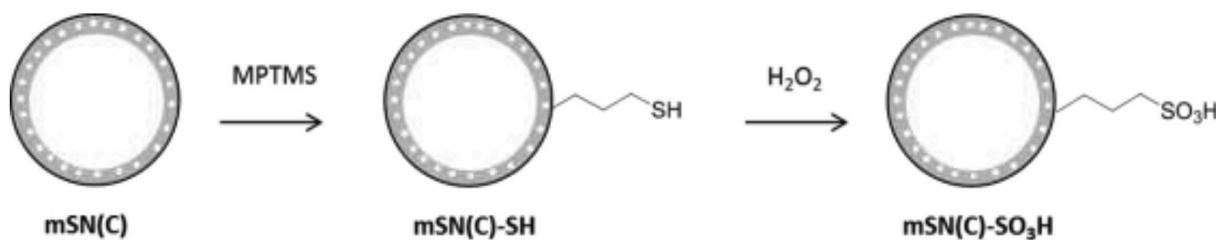


Fig. 5. Synthetic route for acidic mesoporous silica nanocapsules (noted mSN(C)-SO₃H).

was evaluated by Boehm titration at 164 mmol/100g. This value appears unchanged in comparison with the non-functionalized mSN(C) material (171 mmol/100g). Nevertheless, in the case of mSN(C) solid, the acidity value obtained is only due to a high density of surface silanol groups which is not the case for mSN(C)-SO₃H, as proven by XPS. Finally, specific surface area of the acidic material has decreased (783 m²/g) in comparison with mSN(C) starting material (1213 m²/g) suggesting that the sulfonic moieties were not only grafted on the external surface of mSN(C) solid, but were also incorporated inside the porous network. The isotherms curves shape of mSN(C) and mSN(C)-SO₃H materials are similar (ESI 13). Moreover, the DFT analysis shows mesopores for the acidic material (ESI 13), proving that the porous network is still accessible. It can also be observed that the micropores/mesopores ratio increases after the grafting of sulfonic acid groups, and the average mesopores sizes is slightly smaller, which is in agreement with the above considerations of inner surface functionalization inside mesopores.

To evaluate the catalytic performance of the synthesized acidic material, a blank test without catalyst was firstly carried out (Table 2, entry 1). As expected, relatively low conversion and glucose yield were obtained (18% and 15%) meaning that strong acids sites are needed to hydrolyse cellobiose. Indeed, the pure silica material, mSN(C) does not produce any glucose (entry 2). On the contrary, when the acid catalyst was used (entry 3), the conversion was greatly improved (80%) with selectivity of 100% towards the glucose. This result can be assigned to the presence of strong acid sites onto the surface of mSN(C)-SO₃H

Table 2

Conversion and glucose yield for the hydrolysis of cellobiose after 2 h reaction at 130 °C.

	Catalyst	Cellobiose conversion (%)	Glucose yield (%)
1	Blank	18	15
2	mSN(C)	38	0
3	mSN(C)-SO ₃ H	80	80

material, demonstrating its usefulness in the context of biomass conversion. Unfortunately, XPS reveals loss of sulphur by leaching during the catalytic test, which is an ongoing problem for sulfonated silicas in cellobiose hydrolysis [41]. This drawback might be mitigated by changing the solvent used for the reaction. Nevertheless, considering the high specific surface area of our materials (up to 1500 m²/g), the short diffusional pathway and the grafting of sulfonic acid groups into the mesoporous silica framework, they represent an interesting alternative to conventional methods for the preparation of highly functionalized silica-based catalysts. Indeed, solid silica nanospheres having similar diameter as our silica nanocapsules (45.6 nm), display comparatively much lower specific surface area (278 m²/g according to N₂ physisorption measurement) and micropores (pore size distribution centered on 0.8 nm) rather than mesopores. Micropores are too small to graft MPTMS moieties inside them, meaning that a part of the 278 m²/g surface would be useless in solid spherical nanoparticles in the current context. Consequently, for the same engaged mass of acidic catalyst, our mSN(C)-SO₃H material should reach better cellobiose conversion, because it provides more acidic active sites.

4. Conclusions

In this work, we have demonstrated that by using hard and soft dual templates, very different mesoporous silica nanocapsules with a high specific surface area can be successfully prepared. Three parameters have been modified (pH, soft template nature and hard template nature) to prepare materials with variable but controlled properties. XPS and N₂ physisorption confirmed the production of mesoporous silica materials. TEM images have shown that after the calcination step the obtained mesoporous silica nanofibers (when starting from CNF) and mesoporous silica nanospheres (when starting from CB) maintained the hard templates structures, while presenting a thin nanostructured shell with short diffusion pathway for mass transfer. XRD measurements highlighted the

crystalline or amorphous nature of the materials mainly related to the surfactant nature: anionic surfactant giving more ordered materials than neutral surfactant. On the contrary, the nature of hard template does not affect the textural properties of prepared materials. All these results demonstrate that the present strategy could easily be extended to produce other materials, by selecting other pairs of hard/soft templates, giving a whole family of innovative siliceous materials with very high surface areas, together with short and accessible mesopores, that are very useful in many application fields such as catalysis. As an illustration, an acidic material based on the mesoporous silica nanospheres was prepared, characterized and evaluated in a biomass model-reaction: the hydrolysis of cellobiose into glucose. High yield of glucose was obtained (80%), in comparison with a blank test (18%), with 100% selectivity. This result reveals again the potential of the present methodology to produce materials useful in a wide range of applications.

Declaration of competing interest

The authors declare that they have no known competing financial interests or personal relationships that could have appeared to influence the work reported in this paper.

CRediT authorship contribution statement

Tommy Haynes: Conceptualization, Methodology, Investigation, Writing - original draft. **Oujidane Bougnouch:** Investigation. **Vincent Dubois:** Conceptualization, Writing - review & editing. **Sophie Hermans:** Conceptualization, Writing - review & editing, Supervision, Project administration, Funding acquisition.

Acknowledgements

We acknowledge the FRS-FNRS and Université catholique de Louvain for funding. We are grateful to Jean-François Statsijns for technical assistance. We also thank the IMERYS GRAPHITE & CARBON (Belgium) and Applied Sciences Inc. (USA) firms for generous donations of carbon black and carbon nanofibers, respectively.

Appendix A. Supplementary data

Supplementary data to this article can be found online at <https://doi.org/10.1016/j.micromeso.2020.110400>.

References

- C.T. Kresge, M.E. Leonowicz, W.J. Roth, J.C. Vartuli, J.S. Beck, Ordered mesoporous molecular sieves synthesized by a liquid-crystal template mechanism, *Nature* 359 (1992) 710–712, <https://doi.org/10.1038/359710a0>.
- J.S. Beck, J.C. Vartuli, W.J. Roth, M.E. Leonowicz, C.T. Kresge, K.D. Schmitt, C.T. W. Chu, D.H. Olson, E.W. Sheppard, S.B. McCullen, J.B. Higgins, J.L. Schlenker, A new family of mesoporous molecular sieves prepared with liquid crystal templates, *J. Am. Chem. Soc.* 114 (1992) 10834–10843, <https://doi.org/10.1021/ja00053a020>.
- P.N.E. Diagboya, E.D. Dikio, Silica-based mesoporous materials; emerging designer adsorbents for aqueous pollutants removal and water treatment, *Microporous Mesoporous Mater.* 266 (2018) 252–267, <https://doi.org/10.1016/j.micromeso.2018.03.008>.
- Y. Zhou, G. Quan, Q. Wu, X. Zhang, B. Niu, B. Wu, Y. Huang, X. Pan, C. Wu, Mesoporous silica nanoparticles for drug and gene delivery, *Acta Pharm. Sin. B* 8 (2018) 165–177, <https://doi.org/10.1016/j.apsb.2018.01.007>.
- H. Rao, X. Wang, X. Du, Z. Xue, Mini review: electroanalytical sensors of mesoporous silica materials, *Anal. Lett.* 46 (2013) 2789–2812, <https://doi.org/10.1080/00032719.2013.816962>.
- M. Misson, H. Zhang, B. Jin, Nanobiocatalyst advancements and bioprocessing applications, *J. R. Soc. Interface* 12 (2015) 20140891, <https://doi.org/10.1098/rsif.2014.0891>.
- K.S. Rao, K. El-Hami, T. Kodaki, K. Matsushige, K. Makino, A novel method for synthesis of silica nanoparticles, *J. Colloid Interface Sci.* 289 (2005) 125–131, <https://doi.org/10.1016/j.jcis.2005.02.019>.
- X.-D. Wang, Z. Shen, T. Sang, X. Cheng, M. Li, L. Chen, Z. Wang, Preparation of spherical silica particles by Stober process with high concentration of tetra-ethyl-

- orthosilicate, *J. Colloid Interface Sci.* 341 (2010) 23–29, <https://doi.org/10.1016/j.jcis.2009.09.018>.
- T. Jesionowski, Preparation of spherical silica in emulsion systems using the co-precipitation technique, *Mater. Chem. Phys.* 113 (2009) 839–849, <https://doi.org/10.1016/j.matchemphys.2008.08.067>.
- S.K. Park, K. Do Kim, H.T. Kim, Preparation of silica nanoparticles: determination of the optimal synthesis conditions for small and uniform particles, *Colloid. Surface. Physicochem. Eng. Aspect.* 197 (2002) 7–17, [https://doi.org/10.1016/S0927-7757\(01\)00683-5](https://doi.org/10.1016/S0927-7757(01)00683-5).
- M. Marini, B. Pourabbas, F. Pilati, P. Fabbri, Functionally modified core-shell silica nanoparticles by one-pot synthesis, *Colloid. Surface. Physicochem. Eng. Aspect.* 317 (2008) 473–481, <https://doi.org/10.1016/j.colsurfa.2007.11.022>.
- W.Y.D. Yong, Z. Zhang, G. Cristobal, W.S. Chin, One-pot synthesis of surface functionalized spherical silica particles, *Colloid. Surface. Physicochem. Eng. Aspect.* 460 (2014) 151–157, <https://doi.org/10.1016/j.colsurfa.2014.03.039>.
- Y. Ren, G. Zhou, P. Cao, Preparations and properties of a tunable void with shell thickness SiO₂@SiO₂ core-shell structures via activators generated by electron transfer for atom transfer radical polymerization, *Solid State Sci.* 52 (2016) 154–162, <https://doi.org/10.1016/j.solidstatesciences.2015.12.021>.
- B. Wen, C.Q. Huo, C.H. Li, L. Zhang, Preparation of the silica micro-spheres by chemical precipitation process, *Adv. Mater. Res.* 602–604 (2012) 259–264, <https://doi.org/10.4028/www.scientific.net/AMR.602-604.259>.
- S.B. Yoon, J.-Y. Kim, J.H. Kim, Y.J. Park, K.R. Yoon, S. Park, J.-S. Yu, Synthesis of monodisperse spherical silica particles with solid core and mesoporous shell: mesopore channels perpendicular to the surface, *J. Mater. Chem.* 17 (2007) 1758, <https://doi.org/10.1039/b617471j>.
- Y.H. Zhang, Y. Deng, Y.H. Cai, W. Xiao, L.L. Sun, Simple synthesis for hierarchical SiO₂ tubes with adjustable Mesoporous, in: *Proc. 2015 Int. Conf. Power Electron. Energy Eng.*, Atlantis Press, Paris, France, 2015, pp. 215–218, <https://doi.org/10.2991/peeec-15.2015.57>.
- B. Wang, C. Chi, W. Shan, Y. Zhang, N. Ren, W. Yang, Y. Tang, Chiral mesostructured silica nanofibers of MCM-41, *Angew. Chem. Int. Ed.* 45 (2006) 2088–2090, <https://doi.org/10.1002/anie.200504191>.
- S. Bian, Z. Ma, L. Zhang, F. Niu, W. Song, Silica nanotubes with mesoporous walls and various internal morphologies using hard/soft dual templates, *Chem. Commun.* 10 (2009) 1261–1263, <https://doi.org/10.1039/b821196e>.
- X. Wang, H. Fan, P. Ren, H. Yu, J. Li, A simple route to disperse silver nanoparticles on the surfaces of silica nanofibers with excellent photocatalytic properties, *Mater. Res. Bull.* 47 (2012) 1734–1739, <https://doi.org/10.1016/j.materresbull.2012.03.042>.
- H. He, J. Wang, X. Li, X. Zhang, W. Weng, G. Han, Silica nanofibers with controlled mesoporous structure via electrospinning: from random to orientated, *Mater. Lett.* 94 (2013) 100–103, <https://doi.org/10.1016/j.matlet.2012.12.032>.
- Y. Zhou, W.P. Zhang, G. Wang, Y.Q. Zhang, J.H. Cao, D.Y. Wu, Effect of cosurfactants on pore sizes of continuous highly ordered mesoporous silica nanofibers, *Appl. Mech. Mater.* 597 (2014) 13–16, <https://doi.org/10.4028/www.scientific.net/AMM.597.13>.
- Y. Xie, D. Kocaeve, C. Chen, Y. Kocaeve, Review of research on template methods in preparation of nanomaterials, *J. Nanomater.* 2016 (2016) 1–10, <https://doi.org/10.1155/2016/2302595>.
- W. Li, M. Zhang, J. Zhang, Y. Han, Self-assembly of cetyl trimethylammonium bromide in ethanol-water mixtures, *Front. Chem. China* 1 (2006) 438–442, <https://doi.org/10.1007/s11458-006-0069-y>.
- Y. Wan, Zhao, on the controllable soft-templating approach to mesoporous silicates, *Chem. Rev.* 107 (2007) 2821–2860, <https://doi.org/10.1021/cr068020s>.
- H. Ogihara, S. Takenaka, I. Yamanaka, E. Tanabe, A. Genseki, K. Otsuka, Synthesis of SiO₂ nanotubes and their application as nanoscale reactors, *Chem. Mater.* 18 (2006) 996–1000, <https://doi.org/10.1021/cm051727v>.
- C.A.R. Costa, C.A.P. Leite, F. Galembeck, Size dependence of stober silica nanoparticle microchemistry, *J. Phys. Chem. B* 107 (2003) 4747–4755, <https://doi.org/10.1021/jp027525t>.
- H. Zhang, H. Xu, M. Wu, Y. Zhong, D. Wang, Z. Jiao, A soft-hard template approach towards hollow mesoporous silica nanoparticles with rough surfaces for controlled drug delivery and protein adsorption, *J. Mater. Chem. B* 3 (2015) 6480–6489, <https://doi.org/10.1039/C5TB00634A>.
- F. Guo, Z. Fang, C.C. Xu, R.L. Smith, Solid acid mediated hydrolysis of biomass for producing biofuels, *Prog. Energy Combust. Sci.* 38 (2012) 672–690, <https://doi.org/10.1016/j.peccs.2012.04.001>.
- L. Negahdar, J.U. Oltmanns, S. Palkovits, R. Palkovits, Kinetic investigation of the catalytic conversion of cellobiose to sorbitol, *Appl. Catal. B Environ.* 147 (2014) 677–683, <https://doi.org/10.1016/j.apcatb.2013.09.046>.
- T. Haynes, O. Ersen, V. Dubois, D. Desmecht, K. Nakagawa, S. Hermans, Protecting a Pd/CB catalyst by a mesoporous silica layer, *Appl. Catal. B Environ.* 241 (2019) 1946–1954, <https://doi.org/10.1016/j.apcatb.2018.09.018>.
- W.J. Roth, Facile synthesis of the cubic mesoporous material MCM-48. Detailed study of accompanying phase transformations, *Adsorption* 15 (2009) 221–226, <https://doi.org/10.1007/s10450-009-9161-1>.
- J. Wang, H. Ge, W. Bao, Synthesis and characteristics of SBA-15 with thick pore wall and high hydrothermal stability, *Mater. Lett.* 145 (2015) 312–315, <https://doi.org/10.1016/j.matlet.2015.01.113>.
- R.E. Morsi, R.S. Mohamed, Nanostructured mesoporous silica: influence of the preparation conditions on the physical-surface properties for efficient organic dye uptake, *R. Soc. Open Sci.* 5 (2018) 172021, <https://doi.org/10.1098/rsos.172021>.
- P.T. Tanev, T.J. Pinnavaia, Mesoporous silica molecular sieves prepared by ionic and neutral surfactant templating: a comparison of physical properties, *Chem. Mater.* 8 (1996) 2068–2079, <https://doi.org/10.1021/cm950549a>.

- [35] G.J. de, A.A. Soler-Illia, E.L. Crepaldi, D. Grosso, C. Sanchez, Block copolymer-templated mesoporous oxides, *Curr. Opin. Colloid Interface Sci.* 8 (2003) 109–126, <https://doi.org/10.1016/S1359-0294>.
- [36] M. Thommes, K. Kaneko, A. V Neimark, J.P. Olivier, F. Rodriguez-Reinoso, J. Rouquerol, K.S.W. Sing, Physisorption of gases, with special reference to the evaluation of surface area and pore size distribution (IUPAC Technical Report), *Pure Appl. Chem.* 87 (2015) 1051–1069, <https://doi.org/10.1515/pac-2014-1117>.
- [37] J. Villarroel-Rocha, D. Barrera, A. Blanco, M. Jalil, K. Sapag, Importance of the α -plot method in the characterization of nanoporous materials, *Adsorpt. Sci. Technol.* 31 (2013) 165–183, <https://doi.org/10.1260/0263-6174.31.2-3.165>.
- [38] A. Silvestre-Albero, E.O. Jardim, E. Bruijn, V. Meynen, P. Cool, A. Sepúlveda-Escribano, J. Silvestre-Albero, F. Rodríguez-Reinoso, Is there any microporosity in ordered mesoporous silicas? *Langmuir* 25 (2009) 939–943, <https://doi.org/10.1021/la802692z>.
- [39] S. Shylesh, S. Sharma, S. Mirajkar, A. Singh, Silica functionalised sulphonic acid groups: synthesis, characterization and catalytic activity in acetalization and acetylation reactions, *J. Mol. Catal. A Chem.* 212 (2004) 219–228, <https://doi.org/10.1016/j.molcata.2003.10.043>.
- [40] W.N.P. Van Der Graaff, K.G. Olvera, E.A. Pidko, E.J.M. Hensen, Stability and catalytic properties of porous acidic (organo)silica materials for conversion of carbohydrates, *J. Mol. Catal. A Chem.* 388–389 (2014) 81–89, <https://doi.org/10.1016/j.molcata.2013.11.013>.
- [41] M. Karaki, A. Karout, J. Toufaily, F. Rataboul, N. Essayem, B. Lebeau, Synthesis and characterization of acidic ordered mesoporous organosilica SBA-15: application to the hydrolysis of cellobiose and insight into the stability of the acidic functions, *J. Catal.* 305 (2013) 204–216, <https://doi.org/10.1016/j.jcat.2013.04.024>.